# Generation of high-energy 284 ps laser pulse without tail modulation by stimulated Brillouin scattering

**Zhaohong Liu (刘照虹), Yulei Wang (王雨雷)*, Yirui Wang (王一 锐), Hang Yuan (远 航), Zhenxu Bai (白振旭), Hongli Wang (王红丽), Rui Liu (刘 瑞), Sensen Li (李森森), Hengkang Zhang (张恒康), Luoxian Zhou (周罗贤), Tan Tan (谭 谈), Weiming He (何伟明), and Zhiwei Lu (吕志伟)**

*National Key Laboratory of Science and Technology on Tunable Laser, Harbin Institute of Technology, Harbin 150001, China*

**Corresponding author: wyl@hit.edu.cn*

Received March 3, 2016; accepted June 24, 2016; posted online July 15, 2016

We obtain the output of a 284 ps pulse duration without tail modulation based on stimulated Brillouin scattering (SBS) pulse compression pumped by an 8 ns-pulse-duration, 1064 nm-wavelength *Q*-switched Nd:YAG laser. To suppress the tail modulation in SBS pulse compression, proper attenuators, which can control the pump energy within a rational range, are added in a generator-amplifier setup. The experimental result shows that the effective energy conversion efficiency triples when the pump energy reaches 700 mJ to 51%, compared with the conventional generator-amplifier setup.

*OCIS codes: 190.0190, 140.0140.*
*doi: 10.3788/COL201614.091901.*

In recent years, the development of ultrashort-pulse and high-power lasers has been attractive for a wide range of applications, including high harmonic generation with high spectral purity of atomic and molecular spectroscopy[1,2], as efficient pump sources of parametric amplifiers[3,4], and for high spatial resolution in LIDAR Thomson scattering diagnostics[5]. Due to their low pulse energy (a few microjoules), conventional mode-locked lasers with complex schemes[6–8] and microchip lasers with a *Q*-switch[9,10] require further amplification in regenerative and multipass amplifiers that is complicated and has negative effect on the quality of the beam[11]. In comparison with conventional direct amplification, the pulse compression to enhance the peak intensity via a stimulated Brillouin scattering-phase conjugation mirror (SBS-PCM), with its simple structure, low cost, high energy load[12], and arbitrary wavelength operation[13–17], is a promising method.

Since its first observation by Hon[18], SBS pulse compression has made substantial progress in configurations[19–22] and SBS active media[23–25]. For years, researchers' interest in SBS was focused on the acquirement of high-energy, ultrashort pulses and the exploration of SBS media. Marcus compressed a 2.5 ns laser into a 175 ps pulse using a fused quartz[23]. Xu *et al.* demonstrated 40X pulse compression (down to 300 ps) with 1 J using FC-72[24]. Zhu *et al.* demonstrated a temporal compression from 8 ns to 130 ps with an energy of 300 mJ[25]. Feng achieved a 1.2 J, 300 ps compressed duration from a 4 J, 12 ns pulse in water[26].

Despite a good performance, tail modulation of the compressed duration for the practical application of SBS is a big restriction[27]. In the configuration of an SBS generator, tail modulation of the compressed duration occupied a certain proportion in the output energy, and the proportion increased with the increase of the pump power[28]. Previous studies did not differentiate the energy of tail modulation from the output energy. So in fact, the effective output energy of an SBS compressor may not match up to a perceived level in practical applications, and high energy modulation may introduce hidden troubles. On the other hand, tail modulation led to pulse duration broadening after a certain level of growth. Because an SBS generator is an essential component in all current SBS configurations[18,27,28], tail modulation presents an inevitable challenge that must be overcome.

In this Letter, we attribute tail modulation to the increase of the effective pulse duration (described below) and demonstrate an effective pulse duration control technique wherein an attenuator before an SBS generator is used to weaken the pump energy to a rational range. A generator-amplifier setup with different attenuators is conducted in order to confirm the analysis and method.

Tail modulation in high-energy SBS compression is due to insufficient amplification of the Stokes leading edge, and the residual pump pulse amplifies the tail of the Stokes pulse. Previous studies normally use full width at half-maximum (FWHM) to describe the pump duration. Stimulated scattering has distinct threshold characteristics, and only the part of pump pulse that is above a certain threshold intensity is effective for a process of stimulated scattering. Here, in order to describe the process of SBS accurately, for pump radiation, we define the part above the SBS threshold as the effective pulse duration. As shown in Fig. 1, by increasing of the pump energy (power), the time exceeding the SBS threshold moves forward from point "*f*" to point "*b*," and the effective pump duration ($\Delta t$) is $\Delta t_1$, $\Delta t_2$, $\Delta t_3$, and $\Delta t_4$ accordingly. For a given Gaussian laser, the FWHM is a fixed value, while

 

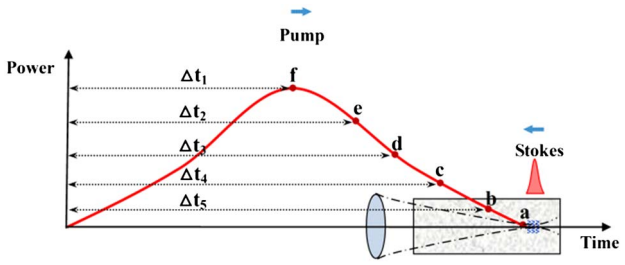


Fig. 1. Illustration of effective pulse duration.

the effective pulse duration ($\Delta t$) changes with the increase of the pump energy, as shown in Fig. 2. The increase of the effective pulse duration leads to a case in which after the Stokes leading edge leaves the active media, the residual pump pulse is intense enough to amplify the Stokes tail. Decreasing the effective pulse duration to an appropriate range is the crux of tail modulation suppression. It is convenient to use an attenuator to decrease the effective pulse duration of the pump directly. Because an attenuator weakens the edge and peak of the Gaussian pulse simultaneously, it is not applicable for the single-cell setup of SBS. As for the generator-amplifier setup, the function of the SBS generator is to provide a Stokes seed, so the use of attenuator to weaken the pump energy of the generator can ensure the conversion efficiency while suppressing the tail modulation.

To verify our analysis, we simulate the process of SBS compression by the classical model[24]. The SBS process involves counter-propagating two optical fields $E_L$ (laser) and $E_S$ (Stokes), which are coupled through electrostriction with an acoustic field $\overline{\rho}$,

$$E_L(z,t) = E_L(z,t)e^{i(k_L z-\omega_L t)} + \text{c.c.}, \tag{1a}$$

$$E_S(z,t) = E_S(z,t)e^{i(-k_S z-\omega_S t)} + \text{c.c.}, \tag{1b}$$

$$\overline{\rho}(z,t) = \rho_0 + \rho(z,t)e^{i(q_B z-\Omega_B t)} + \text{c.c.}. \tag{1c}$$

Optical fields $E_L$ and $E_S$ are governed by Maxwell's equations, and acoustic field $\overline{\rho}$ obeys the Navier–Stokes

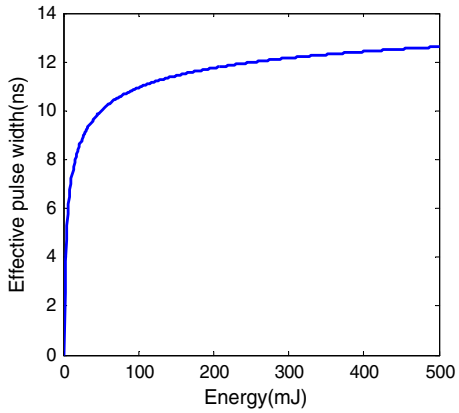


Fig. 2. Effective pulse duration of a Gaussian waveform under different pump energies.

**Table 1.** Physical Properties of FC-72

| Fluorinert property | FC-72 |
|---|---|
| Absorption coefficient ($cm^{-1}$) | $<10^{-3}$ |
| OBT ($GW/cm^2$) | >100 |
| Threshold energy (10 ns, mJ) | 2.5 |
| Brillouin shift (MHz) | 1100 |
| SBS gain coefficient (cm/GW) | 6 |
| Brillouin linewidth (MHz) | 270 |
| Phonon lifetime (ns) | 1.2 |

equation. The wave equations can be written in the forms of Eqs. (2a)–(2c). We solve the Eqs. (2a)–(2c) numerically by a generalization of the split-step method:

$$\frac{\partial E_L}{\partial z} + \frac{\alpha}{2}E_L + \left(\frac{n}{c}\right)\frac{\partial E_L}{\partial t} = \frac{i\omega_L \gamma^e}{2nc\rho_0}\rho E_S, \tag{2a}$$

$$-\frac{\partial E_S}{\partial z} + \frac{\alpha}{2}E_S + \left(\frac{n}{c}\right)\frac{\partial E_S}{\partial t} = \frac{i\omega_S \gamma^e}{2nc\rho_0}\rho^* E_L, \tag{2b}$$

$$\frac{\partial^2 \rho}{\partial t^2} - (2i\omega - \Gamma_B)\frac{\partial \rho}{\partial t} - (i\omega\Gamma_B)\rho = \frac{\gamma^e}{4\pi} q_B^2 E_L E_S^*. \tag{2c}$$

We numerically simulate the Stokes waveform in 700 mJ (maximization output energy of our laser device) with different attenuation ratios. FC-72 is chosen as the active medium. The lengths of cell1 and cell2 are 80 and 60 cm in the simulation, respectively. The parameters of FC-72 are listed in Table 1.

The calculated waveforms in 700 mJ with different attenuation ratios are shown in Fig. 3. It can be seen that the tail modulation is suppressed and maximum power is achieved when a 50% attenuator is used.

The schematic layout is shown in Fig. 4. A $Q$-switched, injection-seeded Nd:YAG laser (Continuum PRII9010) at 1064 nm is operated in a single longitudinal mode; its pulse duration is 8 ns, and its repetition is 1 Hz. A combination of a half-wave plate and a polarizer $P_1$ is used as a variable attenuator. The experimental situation is a generator-amplifier setup, where the laser beam is focused by a 30 cm lens (L) in FC-72 as a Brillouin active medium. The lengths of cell1 and cell2 are 80 and 60 cm, respectively.

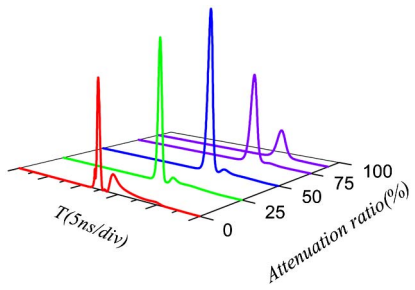


Fig. 3. Calculated waveform at 700 mJ with different attenuation ratios.

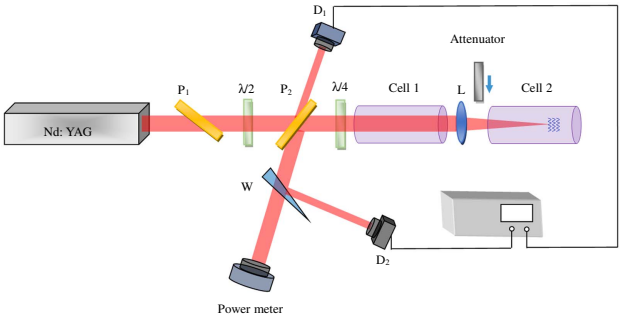


Fig. 4. Schematic of the experimental compressor using a generator-amplifier setup. $P_1$, $P_2$, thin-film polarizer; L, lens; $\lambda/2$, half-wave plate; $\lambda/4$, quarter-wave plate; D1, D2, photodiode.

Between L and cell2, attenuators with different attenuation ratios are used to control the effective pulse duration in the SBS generator (cell 1). A polarization isolator, composed of a polarizer $P_2$ and a quarter-wave plate, is utilized to prevent backward Stokes from penetrating the laser cavity. The waveforms of the pump radiation and backward Stokes were detected by a PIN photodiode (New Focus Vis-IR) $D_1$, $D_2$, and a digital oscilloscope TDS3032B. The output energy was measured by an energy detector ED500 from Israel Ophir.

It is important to note that the process of SBS temporal pulse compression is determined by the configuration of optics, pump laser parameters (linewidth, intensity, and beam quality) and medium parameters (acoustical duration and SBS gain coefficient). In a given condition, the effects of the attenuator can be observed by a set of comparative experiments. In the experiment, we just changed the attenuation ratio (0%, 25%, and 50%).

Figure 5 shows the output pulse duration under different attenuation conditions as a function of the input pump energy. The compressed duration decreases quickly as the input energy increases and saturates gradually to a stable value when the input energy exceeds 500 mJ. At low pump energies (below 300 mJ), the compressor with the lowest attenuation ratio achieved a better compression ratio. Because the attenuator weakens the edge and peak of the seed pulse simultaneously, the Stokes seed is too weak to extract the pump fully. As the input energy increases,

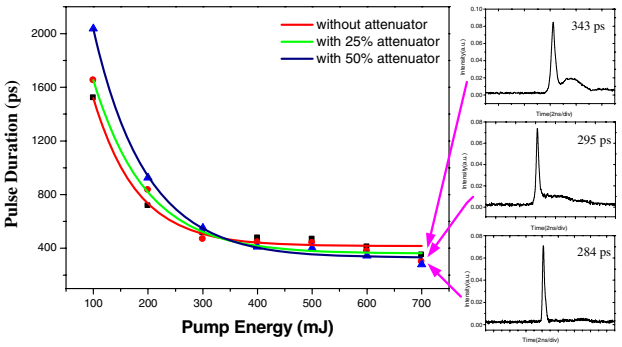


Fig. 5. Pulse duration evolution of output Stokes with respect to input energy using different attenuators. Three insets show compressed pulse shapes in 700 mJ with different attenuation ratios.

tail modulation becomes a main factor of further compression. Modest attenuation before SBS generator can maintain an effective pulse duration in the proper range and suppress the tail modulation. As shown in inset of Fig. 3, the compressed pulse durations with attenuations of 0%, 25%, and 50% are 343, 295, and 284 ps, respectively. Tail modulation suppression can increase the compression ratio to some extent. For a traditional generator-amplifier setup without an attenuator, severe tail modulation is produced. The use of the 25% attenuator can suppress tail modulation to a large extent, and the 50% attenuator can achieve complete suppression at a pump energy of 700 mJ. It should be noted that, if modest attenuation is used, we can achieve a compressed pulse without tail modulation in a large range of input energies (between the thresholds of SBS and SRS for a given active medium[26]).

The ratio of output energy to pump energy is normally used to describe the conversion efficiency of SBS. But the output energy included the energy of both the Stokes main peak and tail modulation. Here, we define the ratio of the main peak energy of the Stokes to the pump energy as the effective energy conversion efficiency. In the experiment, we can achieve the effective energy conversion efficiency through the area ratio of the Stokes main peak to the tail modulation in waveform. Figure 6(a) shows the SBS conversion efficiency according to the conventional definition. In the experiment, the SBS conversion efficiency increases as the pump energy increases and saturates to a maximum value. The compression duration using a lower attenuation achieves a higher SBS conversion efficiency. If we do not include the energy of the tail modulation in the calculations of the SBS conversion efficiency, the effective energy conversion efficiency is as shown in Fig. 6(b). The effective energy conversion efficiency of the setup without an attenuator has a sustained downward trend in the range of 100–700 mJ. An upward SBS compression conversion efficiency with a downward effective energy conversion efficiency means an energy growth of the tail modulation. When the pump energy reaches 700 mJ, the effective energy conversion efficiency is only 14.95%. The effective energy conversion efficiency curve of the setup with the 25% attenuator takes a "saddle pattern" with the increase of the pump energy. This implies that the 25% attenuator can control the generation of tail modulation effectively when the pump energy is lower than 400 mJ. The effective pulse duration increase caused by the higher energy is beyond the capability of the 25% attenuator. Although the 25% attenuator cannot suppress the modulation completely in the case of high pump energy, it raises the effective energy conversion efficiency compared with the situation in which no attenuator is used. The effective energy conversion efficiency of the setup with the 50% attenuator continues to rise in the energy range of 100–700 mJ. Combined with the waveform in Fig. 5, the 50% attenuator shows a good suppression of the tail modulation, and the effective energy conversion efficiency is 51% (output energy: 357 mJ) at a pump energy of 700 mJ. It must be said, though, that the

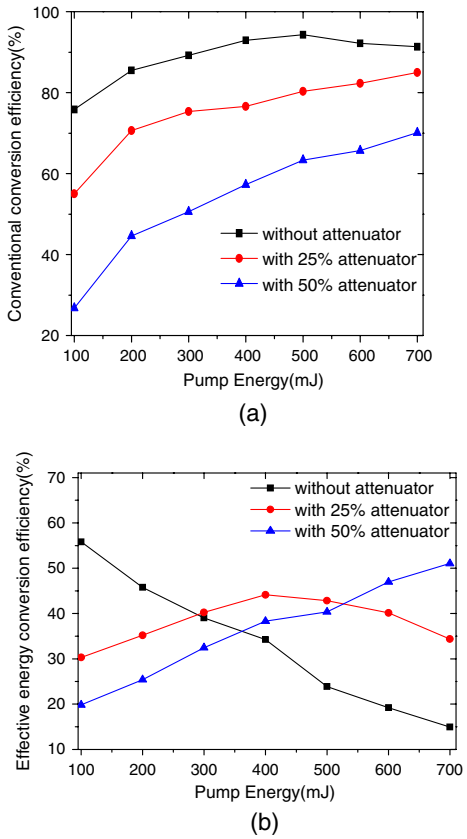


Fig. 6. SBS compression conversion efficiency using several attenuators. (a) Conventional conversion efficiency, which does not eliminate the tail modulation. (b) Effective energy conversion efficiency in which the energy of the tail modulation is not included in the calculations.

attenuation ratio is not "the higher, the better." When the pump energy is lower than 300 mJ, the setup with the lowest attenuation ratio shows a higher effective energy conversion efficiency. So if the effective pump duration is in a rational range, higher attenuation may result in a low effective energy conversion efficiency. In a practical application, it is convenient to use a variable attenuator for an optimal suppression of the SBS tail modulation.

In conclusion, we investigate a method of effective pump duration control of an SBS generator to suppress tail modulation of the output compressed pulse. It is demonstrated that the proper attenuator can control the effective pump duration in an appropriate range as the pump energy increases. Moreover, it is shown that we suppress the tail modulation completely at a pump energy of 700 mJ and achieve a 284 ps pulse duration in FC-72, while the effective energy conversion efficiency is 51% (output energy: 357 mJ).

This work was supported by the National Natural Science Foundation of China (Nos. 61378007 and 61138005) and the Fundamental Research Funds for the Central Universities (No. HIT. IBRSEM. A. 201409).

## References

1. M. Bertolotti, Contemp. Phys. **56**, 88 (2015).
2. R. A. Ganeev, M. Suzuki, and H. Kuroda, Phys. Plasmas **21**, 053503 (2014).
3. T. Popmintchev, M. C. Chen, D. Popmintchev, P. Arpin, S. Brown, S. Alisauskas, G. Andriukaitis, T. Balciunas, O. D. Mücke, A. Pugzlys, A. Baltuska, B. Shim, S. E. Schrauth, A. Gaeta, C. Hernández-García, L. Plaja, A. Becker, A. Jaron-Becker, M. M. Murnane, and H. C. Kapteyn, Science **336**, 1287 (2012).
4. N. Ishii, L. Turi, V. S. Yakovlev, T. Fuji, F. Krausz, A. Baltuska, R. Butkus, G. Veitas, V. Smilgevicius, R. Danielius, and A. Piskarskas, Opt. Lett. **30**, 567 (2005).
5. M. J. Walsh, M. Beurskens, P. G. Carolan, M. Gilbert, M. Loughlin, A. W. Morris, V. Riccardo, Y. Xue, R. B. Huxford, and C. I. Walker, Rev. Sci. Instrum. **77**, 10E525 (2006).
6. J. Au, Aus Der, G. J. Spühler, T. Südmeyer, R. Paschotta, R. HoVel, M. Moser, S. Erhard, M. Karszewski, A. Giesen, and U. Keller, Opt. Lett. **25**, 859 (2000).
7. T. Beddard, W. Sibbett, D. T. Reid, J. Garduno-Mejia, N. Jamasbi, and M. Mohebi, Opt. Lett. **24**, 163 (1999).
8. Z. Liu and S. Izumida, Appl. Phys. Lett. **74**, 3622 (1999).
9. B. Braun, F. X. Kärtner, Rtner, G. Zhang, M. Moser, and U. Keller, Opt. Lett. **22**, 381 (1997).
10. J. J. Zayhowski and C. Dill, Opt. Lett. **19**, 1427 (1994).
11. I. Musgrave, A. Boyle, R. J. Clarke, R. Heathcote, M. Galimberti, D. Neely, M. M. Notley, A. K. K. Pepler, C. Hernandez-Gomez, and L. John, Proc. SPIE **8780**, 8780A (2013).
12. E. Guillaume, K. Humphrey, H. Nakamura, R. M. G. M. Trines, R. Heathcote, M. Galimberti, Y. Amano, D. Doria, G. Hicks, and E. Higson, High Power Laser Sci. Eng. **2**, e33 (2014).
13. H. Yuan, Z. W. Lu, Y. L. Wang, Z. X. Zheng, and Y. Chen, Laser Part. Beams **32**, 369 (2014).
14. W. Hasi, H. Zhao, D. Lin, W. He, and Z. Lu, Chin. Opt. Lett. **13**, 061901 (2015).
15. V. A. Gorbunov, S. B. Papernyĭ, V. F. Petrov, and V. R. Startsev, Sov. J. Quantum Electron. **13**, 900 (1983).
16. D. N. G. Roy and D. V. G. L. N. Rao, J. Appl. Phys. **59**, 332 (1986).
17. K. F. Shipilov and T. A. Shmaonov, Sov. J. Quantum Electron. **16**, 1402 (1986).
18. D. T. Hon, IEEE J. Quantum Electron. **5**, 2396 (1980).
19. Y. Nizienko, A. Mamin, P. Nielsen, and B. Brown, Rev. Sci. Instrum. **65**, 2460 (1994).
20. C. B. Dane, W. A. Neuman, and L. A. Hackel, IEEE J. Quantum Electron. **30**, 1907 (1994).
21. A. Offenberger, D. C. Thompson, R. Fedosejevs, and B. Harwood, IEEE J. Quantum Electron. **29**, 207 (1993).
22. S. Schiemann, W. Ubachs, and W. Hogervorst, IEEE J. Quantum Electron. **33**, 358 (1997).
23. G. Marcus, S. Pearl, and G. Pasmanik, J. Appl. Phys. **103**, 103105 (2008).
24. X. Xiaozhen, F. Chengyong, and D. Jean-Claude, Opt. Express **22**, 13904 (2014).
25. X. Zhu, Z. Lu, and Y. Wang, Laser Part. Beams **33**, 11 (2015).
26. F. Chengyong, X. Xiaozhen, and D. Jean-Claude, Opt. Lett. **39**, 3367 (2014).
27. Y. Hidetsugu, H. Takaki, F. Hisanori, N. Masahiro, and K. Shigeru, Opt. Express **17**, 13654 (2009).
28. E. Takahashi, K. Kuwahara, Y. Matsumoto, I. Okuda, I. Matsushima, S. Kato, and Y. Owadano, Opt. Commun. **185**, 431 (2000).